

# On some geometric features of the Kramer interior solution for a rotating perfect fluid

F.J. Chinae and M.J. Pareja  
 Dept. de Física Teórica II, Ciencias Físicas,  
 Universidad Complutense de Madrid  
 E-28040 Madrid, Spain

## Abstract

Geometric features (including convexity properties) of an exact interior gravitational field due to a self-gravitating axisymmetric body of perfect fluid in stationary, rigid rotation are studied. In spite of the seemingly non-Newtonian features of the bounding surface for some rotation rates, we show, by means of a detailed analysis of the three-dimensional spatial geodesics, that the standard Newtonian convexity properties do hold. A central role is played by a family of geodesics that are introduced here, and provide a generalization of the Newtonian straight lines parallel to the axis of rotation.

PACS numbers: 04.20.Jb, 04.40.-b

## 1 Introduction

In the (thus far, unfulfilled) quest for a realistic exact solution in general relativity, representing both the exterior and interior gravitational field generated by a self-gravitating axisymmetric mass of perfect fluid in stationary rotation, the detailed analysis of the features of whatever partial results we already have seem relevant. Specifically, comparison with the known results in the Newtonian domain will improve our intuition within the general relativistic regime.

It is remarkable that there exists a number of treatments based on numerical integration of the field equations, or on approximation schemes valid for small rotation rates (applied, in particular, for the calculation of the shape of the bounding surface of the fluid configurations, or for the analysis of the meaning of centrifugal forces), but, surprisingly, very few exact results, based on the growing wealth of interior exact solutions in the literature (both rigidly and differentially rotating). In the present paper, we analyze some geometric features of one such interior solution, in order to check whether the analog of some Newtonian properties hold. Remarkably, they do, in spite of the fact that the analysis of the bounding surface  $p = 0$  in Section 3 naively seems to point to the contrary.

A more detailed analysis of the three-dimensional geodesics (Sections 4 and 5) shows that standard Newtonian features indeed hold for the solution under consideration, if some of the Newtonian elements are redefined appropriately. In particular, we introduce in Section 5 what we believe is the generalization of straight lines parallel to the rotation axis in the Newtonian case: Geodesics whose points have constant azimuthal angle and intersect the equatorial plane orthogonally.

## 2 The Kramer solution

An exact solution of the Einstein field equations, representing the interior gravitational field of a self-gravitating, axially symmetric, rigidly rotating perfect fluid, was introduced in [1], and was further analyzed in [2]. The metric can be written as

$$2m ds^2 = [\eta - 1 - b \cos \xi e^{-\eta}] dt^2 + [4(\eta - 1) - 4b \cos \xi (e^{-\eta} - e^{-1})] dt d\varphi \quad (1)$$

$$+ [4(\eta - 1) - 4b \cos \xi (e^{-\eta} + e^{\eta-2} - 2e^{-1})] d\varphi^2 + \frac{d\eta^2}{\eta - 1} + \frac{e^\eta}{b \cos \xi} d\xi^2 ,$$

where  $m$  and  $b$  are positive parameters. The coordinate  $t$  is a time coordinate, while  $\varphi$  is an azimuthal angle. The spacetime possesses the two commuting Killing fields  $\partial_t$  and  $\partial_\varphi$ . The axis of rotation is characterized by the equation  $\eta = 1$ , and there exists a discrete symmetry  $\xi \rightarrow -\xi$ . The invariant set under this symmetry (i.e., points with  $\xi = 0$ ) will be referred to as the *equatorial plane* in what follows, and the point with coordinates  $\eta = 1$ ,  $\xi = 0$  as the *center* of the body. The fluid obeys the following barotropic equation of state

$$\varepsilon + 3p = \frac{2m}{\kappa_0} , \quad (2)$$

where  $p$  is the pressure and  $\varepsilon$  the energy density, and  $\kappa_0$  is a positive constant. The dependence on  $\eta$  and  $\xi$  of the pressure and the energy density is the following:

$$p = \frac{m}{2\kappa_0} (1 + \eta - b \cos \xi e^{-\eta}) \quad (3)$$

$$\varepsilon = \frac{m}{2\kappa_0} (1 - 3\eta + 3b \cos \xi e^{-\eta}) . \quad (4)$$

It is rather remarkable that the pressure is harmonic in the  $(\eta, \xi)$  coordinates:

$$p_{\eta\eta} + p_{\xi\xi} = 0 . \quad (5)$$

Due to the minimum principle for the corresponding Laplacian, the pressure attains its minimum value at the boundary of the domain of definition in the  $(\eta, \xi)$  plane. This domain is given by the interior of the region bounded by the line  $\eta = 1$  and the curve  $p(\eta, \xi) = 0$ . As a matter of fact, the pressure has its lowest possible (negative) value at the center. The boundary value  $p = 0$

(the greatest value) defines the boundary of the object. In spite of the pressure being negative inside the body, and growing from the center to the boundary, the dominant energy condition is satisfied:

$$\varepsilon > 0, \quad |p| < \varepsilon . \quad (6)$$

It is remarkable that the boundary  $p = 0$  has a relatively simple equation

$$b \cos \xi - (1 + \eta)e^\eta = 0 . \quad (7)$$

This, and the fact that (as will be shown in Section 4) the integration of the relevant spatial geodesics can be reduced to quadratures, is crucial in our analysis of the geometric features of the solution.

The parameter  $b$  is related to the modulus of the vorticity vector at the center by means of

$$(\omega_\mu \omega^\mu)^{\frac{1}{2}} = \sqrt{\frac{m}{2be}}(b + e) . \quad (8)$$

When the requirement is made that the metric have the appropriate signature, as well as the requirement that  $\partial_t$  be timelike and  $\partial_\varphi$  spacelike, the following inequalities result [1]:

$$m > 0, \quad \eta \geq 1, \quad b \cos \xi > 0, \quad 1 - \eta + b \cos \xi e^{-\eta} > 0, \quad (\eta + 1)(2e^{\eta-1} - e^{2\eta-2}) \geq 2 . \quad (9)$$

We shall refer to the intersection of the equatorial plane with the boundary  $p = 0$  as the *equator* of the body, and to the region with  $\xi > 0$  (respectively,  $\xi < 0$ ) as the *northern* (resp., *southern*) *hemisphere*. Similarly, the intersection of the axis of rotation with the boundary  $p = 0$  having  $\xi > 0$  will be called the *north pole*; the intersection with  $\xi < 0$  will be termed the *south pole*. The object is oblate (in the sense that the polar distance to the center is less than the distance from one point in the equator to the center), as calculated in [1].

As  $b$  is bounded away from zero, there is no static limit for this solution. One is tempted to interpret this feature in the light of the Newtonian result [3] that the pressure cannot have a minimum at the center if  $\Omega^2 < 2\pi\rho$ , where  $\Omega$  is the angular velocity of the Newtonian fluid body, and  $\rho$  the mass density. It would be of interest to find the corresponding result in general relativity.

Finally, let us mention that the acceleration and the vorticity vectors are parallel at the pole, and orthogonal at the equator, as required for symmetry reasons.

### 3 Geometry of the bounding surface $t = \text{const.}$ , $p = 0$

The spacetime metric (1) induces the following metric on the two-dimensional surface  $t = \text{const.}$ ,  $p = 0$ :

$$\begin{aligned}
2m ds_2^2 &= g_{\varphi\varphi} d\varphi^2 + g_{\eta\eta} d\eta^2 \\
&= [4(\eta + 1)(2e^{\eta-1} - e^{2\eta-2}) - 8] d\varphi^2 + \frac{b^2(\eta + 1) - (3\eta + 5)e^{2\eta}}{[b^2 - (1 + \eta)^2 e^{2\eta}](\eta^2 - 1)} d\eta^2,
\end{aligned} \tag{10}$$

where we have used the equation for the surface  $p = 0$  (7) in order to express the two-dimensional metric as a function of the coordinate  $\eta$ . It is remarkable that (for large enough values of the rotation parameter  $b$ ) the surface possesses a region around the equator with *negative* Gaussian curvature  $K$  (Figs. 1-2). Our intuition with two-dimensional surfaces embedded in three-dimensional

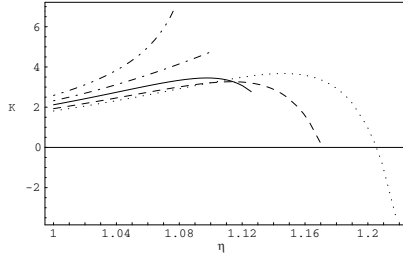


**Figure 1.** Gaussian curvature on the two-surface  $t = \text{const.}$ ,  $p = 0$ , from the pole ( $\eta = 1$ ) to the equator, for different values of the parameter  $b$  ( $b = 6.1, 6.3, 6.5529, 7, 7.5$ ) corresponding, respectively, to the double-dot-dashed, dot-dashed, solid, dashed and dotted lines in the figure. ( $2m = 1$ )

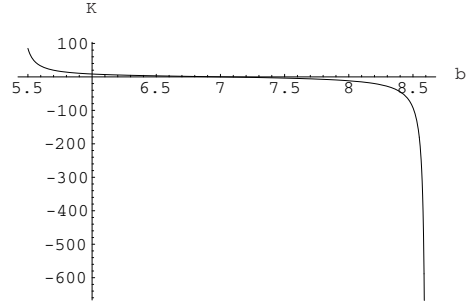


**Figure 2.** Gaussian curvature on the two-surface  $t = \text{const.}$ ,  $p = 0$ , in the equator, as a function of  $b$ .

Euclidean space would lead us to interpret that region as a concave “waist” near the equator. This impression is reinforced by computing the length of the parallels (closed curves of constant  $\eta$ , that circle around the surface and can be parametrized by means of the azimuthal angle; they are not geodesics, in general). The expression for the length of one such parallel, obtained from (10), is the following:

$$l = \sqrt{\frac{2}{m}} \pi [4(\eta + 1)(2e^{\eta-1} - e^{2\eta-2}) - 8]^{\frac{1}{2}}. \tag{11}$$

It is easily seen that the length presents a local maximum for

$$2\eta + 4 - (2\eta + 3)e^{\eta-1} = 0. \tag{12}$$

As a matter of fact, if the length is plotted as a function of  $\eta$  (Fig. 3), we see that it increases monotonically from  $\eta = 1$  (corresponding to the pole, in which case the length vanishes) to a maximum at  $\eta = 1.1716$ , obtained by solving

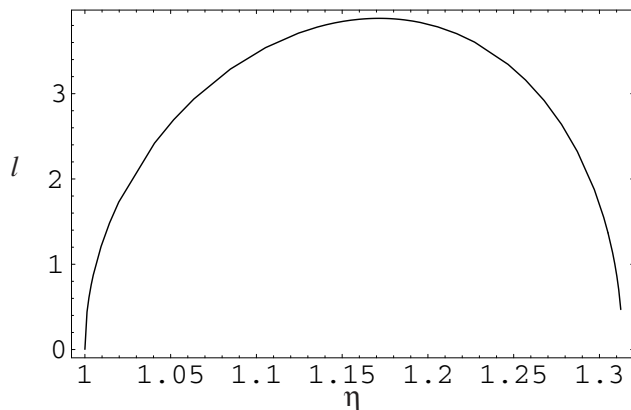


**Figure 3.** Length of the parallels (closed curves of  $\eta = \text{const.}$ , parametrized by  $\varphi$  in the surface  $p = 0$ .)

numerically (12). From that point on, the length decreases, until it vanishes again for the numerical value  $\eta = 1.3134$ . Please notice that the preceding values, as well as (12) itself, do not depend on the rotation parameter  $b$ . The dependence on  $b$ , however, shows up in the following: the coordinate  $\eta$  varies from  $\eta = 1$  (intersection of the rotation axis with the surface  $p = 0$ ) to a maximum value (corresponding to the equator), obtained by solving (7) with  $\xi = 0$ . Accordingly, the maximum value of  $\eta$  is an increasing function of  $b$ . When  $b < 7.0077$ , the corresponding  $\eta$  is such that it falls within the left side of the curve in Fig. 3, and we have the “normal” situation, where the length of the parallels increases from one pole to the equator. But, if  $b > 7.0077$ , then the maximum length for a parallel occurs at an intermediate latitude, and it subsequently decreases towards the equator. In the extreme case  $b = 8.603$  ( $\eta = 1.3134$ ), the circumferential length at the equator vanishes, which could be interpreted as the fission of the body along the equator at the extreme rotation rate. Due to positivity requirements in the metric, the values  $\eta > 1.3134$  are excluded.

The Gaussian curvature of the two-surface vanishes precisely at  $\eta = 1.1716$ . This is not accidental, as the curvature has a factor  $g_{\varphi\varphi,\eta}$ , and  $g_{\varphi\varphi,\eta} = 0$  is precisely the condition expressed by (12). Thus, the surface is “flat” at the equator for  $b = 7.0077$ . If  $b$  is increased, then a finite region with  $K < 0$  arises symmetrically around the equator, including the equator itself. At the extreme value  $b = 8.603$ ,  $K$  becomes singular (minus infinity, see Fig. 2) at the equator.

If the three-geometry where the two-surface  $t = \text{const.}$ ,  $p = 0$  is embedded were Euclidean, we would find that the three-volume  $t = \text{const.}$  enclosed

by the two-surface would not be convex, and, in particular, certain straight lines parallel to the axis of rotation would intersect the boundary  $p = 0$  in more than two points (for sufficiently large values of  $b$ ), against the well-known Newtonian theorems of Lichtenstein, [4], [5], [3]. We shall see below, however, that a natural generalization of the mentioned parallel straight lines to the true three-dimensional Riemannian geometry does preserve the analog of the classical results.

It should be remarked that the closed curves  $\eta = \text{const.}$  on the boundary surface are not geodesics on the surface, except for the particular case where  $g_{\varphi\varphi,\eta} = 0$ . This can be readily seen by writing the equations for the geodesics in the metric (10)

$$g_{\varphi\varphi}\dot{\varphi} = \text{const.} \quad (13)$$

$$2g_{\eta\eta}\ddot{\eta} + g_{\eta\eta,\eta}\dot{\eta}^2 - g_{\varphi\varphi,\eta}\dot{\varphi}^2 = 0 \quad (14)$$

(where a dot denotes a derivative with respect to length along the geodesic).

We thus see that the only parallel circles which are geodesics are the two (symmetrically placed with respect to the equator) corresponding to  $\eta = 1.1716$ , when  $b > 7.0077$ . When  $b = 7.0077$ , the two parallels coincide with the equator (and that is the only case in which the equator is a geodesic).

Finally, it is easily shown (by numerically computing the Gauss-Bonnet integral of  $K$  over the surface) that the two-surface  $t = \text{const.}$ ,  $p = 0$  has the topology of a 2-sphere.

## 4 Geodesics of the three-dimensional spatial metric

The spacetime metric (1) reduces for  $t = \text{const.}$  to the following three-dimensional metric:

$$2m ds_3^2 = 4[\eta - 1 - b \cos \xi (e^{-\eta} + e^{\eta-2} - 2e^{-1})] d\varphi^2 + \frac{d\eta^2}{\eta - 1} + \frac{e^\eta}{b \cos \xi} d\xi^2. \quad (15)$$

From (15), we find the following equations for the geodesics in the three-space:

$$[\eta - 1 - b \cos \xi (e^{-\eta} + e^{\eta-2} - 2e^{-1})] \dot{\varphi} = \text{const.} \quad (16)$$

$$\frac{2\ddot{\eta}}{\eta - 1} - \frac{\dot{\eta}^2}{(\eta - 1)^2} - \frac{e^\eta}{b \cos \xi} \dot{\xi}^2 - 4[1 - b \cos \xi (-e^{-\eta} + e^{\eta-2})] \dot{\varphi}^2 = 0 \quad (17)$$

$$\frac{2e^\eta}{b \cos \xi} \ddot{\xi} + \frac{2e^\eta \dot{\eta} \dot{\xi}}{b \cos \xi} + \frac{e^\eta \sin \xi}{b \cos^2 \xi} \dot{\xi}^2 - 4b \sin \xi (e^{-\eta} + e^{\eta-2} - 2e^{-1}) \dot{\varphi}^2 = 0. \quad (18)$$

In particular, geodesics with  $\dot{\varphi} = 0$  are characterized by the two equations

$$\frac{2\dot{\eta}}{\eta-1} - \frac{\dot{\eta}^2}{(\eta-1)^2} - \frac{e^\eta}{b \cos \xi} \dot{\xi}^2 = 0 \quad (19)$$

$$\ddot{\xi} + \dot{\eta}\dot{\xi} + \frac{1}{2} \frac{\sin \xi}{\cos \xi} \dot{\xi}^2 = 0 . \quad (20)$$

It is a rather remarkable feature of the Kramer solution that the geodesic equations (19)-(20) can be reduced to quadratures. Two clearly different cases appear, depending on whether  $\dot{\xi} = 0$  at all points of the geodesic or not. In the former case, the integration reduces to that of the equation

$$\frac{2\ddot{\eta}}{\eta-1} - \frac{\dot{\eta}^2}{(\eta-1)^2} = 0 , \quad (21)$$

which yields

$$s = q \sqrt{\frac{2}{m}} [\sqrt{\eta_f - 1} - \sqrt{\eta_i - 1}] , \quad (22)$$

where  $q = \pm 1$ , depending on the sense in which the geodesic is traversed;  $\eta_i$  is the initial  $\eta$  coordinate, and  $\eta_f$  the final one, and  $s$  is the distance along the geodesic. In the case  $\dot{\xi} \neq 0$ , we introduce the new variable  $w = \sqrt{\eta - 1}$ , in order to simplify the equations. By dividing eq. (20) by  $\dot{\xi}$ , it can be immediately integrated once, giving

$$\frac{\dot{\xi}^2}{\cos \xi} = k e^{-2\eta} , \quad (23)$$

where  $k$  is a positive constant. By substituting (23) into (19), we get

$$\ddot{w} - \frac{k}{4be} w e^{-w^2} = 0 . \quad (24)$$

If  $\dot{w} = 0$ , we get the system

$$w = 0 \quad (25)$$

$$\frac{\dot{\xi}^2}{\cos \xi} = k e^{-2} . \quad (26)$$

This corresponds to the geodesic along the rotation axis. In the generic case,  $\dot{w} \neq 0$ , upon multiplication of (24) by  $\dot{w}$  we get

$$\ddot{w}\dot{w} - \frac{k}{4be} e^{-w^2} w \dot{w} = 0 , \quad (27)$$

whose first integral is

$$4\dot{w}^2 + \frac{k}{be} e^{-w^2} = \alpha \quad (28)$$

with  $\alpha > 0$  a constant of integration. One can now express the relation among the coordinate  $w$  on the geodesic and the distance  $s$  along the geodesic by

$$\frac{2dw}{\sqrt{\alpha - \frac{k}{be}e^{-w^2}}} = qds \quad (29)$$

( $q = \pm 1$ ), while the equation for the trajectory is given by

$$\frac{d\xi}{\sqrt{\cos \xi}} = 2\epsilon q \frac{\sqrt{k}}{e} \frac{e^{-w^2}}{\sqrt{\alpha - \frac{k}{be}e^{-w^2}}} dw, \quad (30)$$

where  $\epsilon = \pm 1$ . By using (15), we find  $\alpha = 2m$ . To summarize, the relevant equations can be written as

$$\dot{w} = q \sqrt{\frac{m}{2}} \frac{1}{\sqrt{\beta}} \sqrt{\beta - e^{-w^2}} \quad (31)$$

$$\dot{\xi} = 2\epsilon q \sqrt{\frac{m}{2}} \frac{1}{\sqrt{\beta}} \sqrt{\frac{b}{e}} \sqrt{\cos \xi} e^{-w^2} \quad (32)$$

where  $\beta = \frac{be\alpha}{k}$ .

Eqs. (31) and (32) can be expressed as quadratures:

$$\frac{d\xi}{\sqrt{\cos \xi}} = 2\epsilon \sqrt{\frac{b}{e}} \frac{e^{-w^2}}{\sqrt{\beta - e^{-w^2}}} dw \quad (33)$$

$$ds = q \sqrt{\frac{2}{m}} \sqrt{\beta} \frac{dw}{\sqrt{\beta - e^{-w^2}}} \quad (34)$$

(Notice that  $q$  and  $\epsilon$  are signs, which can be chosen so that the distance  $s$  along the geodesic increases from the initial value  $s = 0$  at the initial point.)

## 5 Convexity properties of the fluid body

Given the results in Section 3, one could naively expect that the distance from points in the surface  $p = 0$  to the axis of rotation would decrease (for large enough values of  $b$ ) as the equator is approached. We shall see that this is not the case. In order to do that, let us first identify some general properties of geodesics starting from some point in the symmetry axis and reaching a point in the boundary  $p = 0$ . For definiteness, we shall work in the northern hemisphere; due to the symmetry with respect to the equatorial plane, analogous considerations hold for the southern hemisphere.

The first observation is that geodesics from the axis of rotation lie in the  $(w, \xi)$  plane, with constant  $\varphi$ . This can be seen from eq. (16): If the value  $w = 0$  ( $\eta = 1$ ), characterizing the axis, is substituted, then the left-hand side vanishes. Therefore, the constant on the right vanishes. That shows that  $\dot{\varphi} = 0$



for such geodesics. The relevant equations for the geodesics are then (19)-(20), whose integrals are given by (33)-(34). Next, we find the meaning of the constant  $\beta$ : It is easily seen, by using the standard Riemannian formula, that the angle  $\gamma$  between the axis and the tangent to the geodesic at the axis (defined such that  $\gamma = 0$  for a geodesic starting at the axis and pointing towards the north pole) is related to  $\beta$  by the following relation:

$$\cos \gamma = \frac{1}{\sqrt{\beta}} . \quad (35)$$

For a given point in the boundary  $p = 0$ , characterized by  $w = w_f$ , it is found that a geodesic joining it to the axis has a distance  $s$  to the axis given by

$$s = \sqrt{\frac{2}{m}} \int_0^{w_f} \frac{dw}{\sqrt{1 - \cos^2 \gamma e^{-w^2}}} . \quad (36)$$

From (36), we see that

$$\frac{\partial s}{\partial \gamma} = -\sqrt{\frac{2}{m}} \sin \gamma \cos \gamma \int_0^{w_f} \frac{e^{-w^2}}{(1 - \cos^2 \gamma e^{-w^2})^{\frac{3}{2}}} dw . \quad (37)$$

As a consequence,  $s$  is a decreasing function of  $\gamma$  in the northern hemisphere. The minimum obtains for  $\gamma = \frac{\pi}{2}$ , which corresponds to a geodesic with constant  $\xi$ , whose length (22) is

$$s = \sqrt{\frac{2}{m}} w_f . \quad (38)$$

This, being the minimum of the different distances along different geodesics to the axis, we will define as *the distance to the axis* from the given point  $(w_f, \xi_f)$  in the boundary. Let us now look at how the distance so defined varies when we consider different points in the boundary. By using the equation for the boundary,

$$(w_f^2 + 2)e^{w_f^2} = \frac{b}{e} \cos \xi_f , \quad (39)$$

and the derivative of  $w_f$  with respect to  $\xi_f$  along the boundary,

$$\frac{dw_f}{d\xi_f} = -\left(\frac{b}{e}\right) \frac{e^{-w_f^2}}{2w_f^3 + 6w_f} \cos \xi_f , \quad (40)$$

we get

$$\frac{\partial s}{\partial \xi_f} = \frac{\partial s}{\partial w_f} \frac{dw_f}{d\xi_f} = -\sqrt{\frac{2}{m}} \left(\frac{b}{e}\right) \frac{e^{-w_f^2}}{2w_f^3 + 6w_f} \cos \xi_f , \quad (41)$$

thus showing that the distance from a point in the boundary to the axis *increases* monotonically from the north pole to the equator.

Another measure of the convexity (or lack thereof) of the boundary  $p = 0$  is the behaviour of the distances from the center ( $w = 0, \xi = 0$ ) to points in the boundary (Fig. 4). Let us denote by  $w_f(\gamma)$  the  $w$  coordinate of the endpoint of

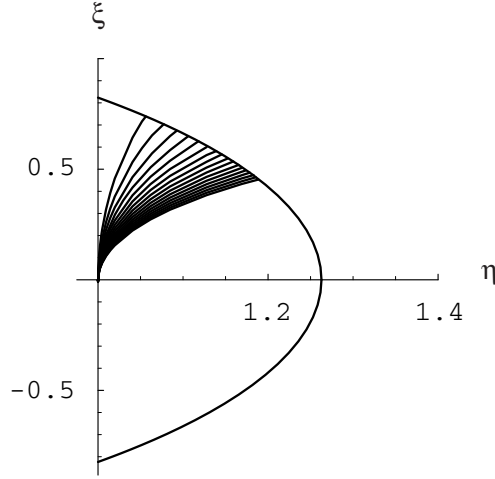


**Figure 4.** Trajectories of geodesics  $\varphi = \text{const.}$  from the center to the surface  $p = 0$ , with different values of initial velocities, i.e., varying  $\beta$

a geodesic starting from the center with an angle  $\gamma$  with respect to the northern semiaxis. The distance to the endpoint will be given by

$$\sqrt{\frac{m}{2}}s = \int_0^{w_f(\gamma)} \frac{1}{\sqrt{1 - \cos^2 \gamma e^{-w^2}}} dw . \quad (42)$$

According to the previous equation, the derivative of  $s$  with respect to  $\gamma$  is

$$\sqrt{\frac{m}{2}} \frac{\partial s}{\partial \gamma} = \frac{\partial w_f(\gamma)}{\partial \gamma} \frac{1}{\sqrt{1 - \cos^2 \gamma e^{-w_f^2(\gamma)}}} - \int_0^{w_f(\gamma)} \frac{\sin \gamma \cos \gamma e^{-w^2}}{(1 - \cos^2 \gamma e^{-w^2})^{\frac{3}{2}}} dw . \quad (43)$$

We are interested in the growth properties of  $s$  at the equator. In order to evaluate the derivative  $\frac{\partial w_f(\gamma)}{\partial \gamma}$ , we consider the equation for the boundary (39), and differentiate it with respect to  $\gamma$ :

$$-\frac{b}{e} \sin \xi_f(\gamma) \frac{\partial \xi_f(\gamma)}{\partial \gamma} = [2w_f^3(\gamma) + 6w_f(\gamma)] e^{w_f^2(\gamma)} \frac{\partial w_f(\gamma)}{\partial \gamma} . \quad (44)$$

The geodesic with  $\gamma = \frac{\pi}{2}$  corresponds to a geodesic along the equatorial plane, with  $\xi = 0$ . Hence,  $\xi_f(\frac{\pi}{2}) = 0$ . Substituting  $\gamma = \frac{\pi}{2}$  in (44), one gets

$$\left[ 2w_f^3\left(\frac{\pi}{2}\right) + 6w_f\left(\frac{\pi}{2}\right) \right] e^{w_f^2(\frac{\pi}{2})} \frac{\partial w_f(\gamma)}{\partial \gamma} \Big|_{\gamma=\frac{\pi}{2}} = 0 . \quad (45)$$

But the coefficient in front of the derivative does not vanish; therefore,

$$\left. \frac{\partial w_f(\gamma)}{\partial \gamma} \right|_{\gamma=\frac{\pi}{2}} = 0 . \quad (46)$$

By substituting this result in eq. (43), evaluated at  $\gamma = \frac{\pi}{2}$ , we get

$$\left. \frac{\partial s}{\partial \gamma} \right|_{\gamma=\frac{\pi}{2}} = 0 , \quad (47)$$

thus showing that the distance from the center to the equator is a local extremum, if the second derivative of  $s$  with respect to  $\gamma$  does not vanish. Its sign will then decide whether the equatorial distance is a maximum (corresponding to local convexity at the equator) or a minimum (local concavity). The second derivative of  $s$  with respect to  $\gamma$  will be given from eq. (43) by

$$\begin{aligned} \sqrt{\frac{m}{2}} \frac{\partial^2 s}{\partial \gamma^2} &= \frac{\partial^2 w_f(\gamma)}{\partial \gamma^2} (1 - \cos^2 \gamma e^{-w_f^2(\gamma)})^{-\frac{1}{2}} - (1 - \cos^2 \gamma e^{-w_f^2(\gamma)})^{-\frac{3}{2}} \times \\ &\quad [\cos \gamma \sin \gamma + \cos^2 \gamma w_f(\gamma)] e^{-w_f^2(\gamma)} \left[ \frac{\partial w_f(\gamma)}{\partial \gamma} \right]^2 \\ &\quad - \sin \gamma \cos \gamma e^{-w_f^2(\gamma)} (1 - \cos^2 \gamma e^{-w_f^2(\gamma)})^{-\frac{3}{2}} \frac{\partial w_f(\gamma)}{\partial \gamma} \\ &\quad + (\sin^2 \gamma - \cos^2 \gamma) \int_0^{w_f(\gamma)} \frac{e^{-w^2}}{(1 - \cos^2 \gamma e^{-w^2})^{\frac{3}{2}}} dw \\ &\quad - 3 \sin^2 \gamma \cos^2 \gamma \int_0^{w_f(\gamma)} \frac{e^{-2w^2}}{(1 - \cos^2 \gamma e^{-w^2})^{\frac{3}{2}}} dw . \end{aligned} \quad (48)$$

At  $\gamma = \frac{\pi}{2}$ , the preceding equation reduces to

$$\left. \sqrt{\frac{m}{2}} \frac{\partial^2 s}{\partial \gamma^2} \right|_{\gamma=\frac{\pi}{2}} = \left. \frac{\partial^2 w_f(\gamma)}{\partial \gamma^2} \right|_{\gamma=\frac{\pi}{2}} + \int_0^{w_f(\frac{\pi}{2})} e^{-w^2} dw . \quad (49)$$

In order to evaluate the second derivative  $\left. \frac{\partial^2 w_f(\gamma)}{\partial \gamma^2} \right|_{\gamma=\frac{\pi}{2}}$ , we first consider the equation for the trajectory of a geodesic from the center; from (33),

$$\int_0^{\xi_f(\gamma)} \frac{d\xi}{\sqrt{\cos \xi}} = 2\sqrt{\frac{b}{e}} \cos \gamma \int_0^{w_f(\gamma)} \frac{e^{-w^2}}{\sqrt{1 - \cos^2 \gamma e^{-w^2}}} dw . \quad (50)$$

By differentiating (50) with respect to  $\gamma$ , we find

$$\begin{aligned} \frac{\partial \xi_f(\gamma)}{\partial \gamma} \frac{1}{\sqrt{\cos \xi_f(\gamma)}} &= 2\sqrt{\frac{b}{e}} \cos \gamma \frac{\partial w_f(\gamma)}{\partial \gamma} \frac{e^{-w_f^2(\gamma)}}{\sqrt{1 - \cos^2 \gamma e^{-w_f^2(\gamma)}}} \\ &\quad - 2\sqrt{\frac{b}{e}} \sin \gamma \int_0^{w_f(\gamma)} \frac{e^{-w^2} dw}{(1 - \cos^2 \gamma e^{-w^2})^{\frac{3}{2}}} . \end{aligned} \quad (51)$$

Hence

$$\left. \frac{\partial \xi_f(\gamma)}{\partial \gamma} \right|_{\gamma=\frac{\pi}{2}} = -2\sqrt{\frac{b}{e}} \int_0^{w_f(\frac{\pi}{2})} e^{-w^2} dw . \quad (52)$$

By differentiating (44) we obtain

$$\begin{aligned} & -\frac{b}{e} \cos \xi_f(\gamma) \left[ \frac{\partial \xi_f(\gamma)}{\partial \gamma} \right]^2 - \frac{b}{e} \sin \xi_f(\gamma) \frac{\partial^2 \xi_f(\gamma)}{\partial \gamma^2} \\ &= \frac{\partial}{\partial w_f(\gamma)} \left\{ [2w_f^3(\gamma) + 6w_f(\gamma)] e^{w_f^2(\gamma)} \right\} \left[ \frac{\partial w_f(\gamma)}{\partial \gamma} \right]^2 \\ &+ [2w_f^3(\gamma) + 6w_f(\gamma)] e^{w_f^2(\gamma)} \frac{\partial^2 w_f(\gamma)}{\partial \gamma^2} , \end{aligned} \quad (53)$$

and, setting  $\gamma = \frac{\pi}{2}$  in (53),

$$-\frac{b}{e} \left[ \left. \frac{\partial \xi_f(\gamma)}{\partial \gamma} \right|_{\gamma=\frac{\pi}{2}} \right]^2 = \left[ 2w_f^3\left(\frac{\pi}{2}\right) + 6w_f\left(\frac{\pi}{2}\right) \right] e^{w_f^2(\frac{\pi}{2})} \left. \frac{\partial^2 w_f(\gamma)}{\partial \gamma^2} \right|_{\gamma=\frac{\pi}{2}} . \quad (54)$$

Finally, from (54) and (52) we get

$$\left. \frac{\partial^2 w_f(\gamma)}{\partial \gamma^2} \right|_{\gamma=\frac{\pi}{2}} = -2 \left( \frac{b}{e} \right)^2 \frac{e^{-w_f^2(\frac{\pi}{2})}}{w_f^3(\frac{\pi}{2}) + 3w_f(\frac{\pi}{2})} \left[ \int_0^{w_f(\frac{\pi}{2})} e^{-w^2} dw \right]^2 . \quad (55)$$

Going back to (49), and substituting  $\left. \frac{\partial^2 w_f(\gamma)}{\partial \gamma^2} \right|_{\gamma=\frac{\pi}{2}}$  from (55), the following expression for the second derivative of the distance is obtained:

$$\sqrt{\frac{m}{2}} \left. \frac{\partial^2 s}{\partial \gamma^2} \right|_{\gamma=\frac{\pi}{2}} = \int_0^{w_f(\frac{\pi}{2})} e^{-w^2} dw \left[ 1 - \frac{2(\frac{b}{e})^2 e^{-w_f^2(\frac{\pi}{2})}}{w_f^3(\frac{\pi}{2}) + 3w_f(\frac{\pi}{2})} \int_0^{w_f(\frac{\pi}{2})} e^{-w^2} dw \right] . \quad (56)$$

But, substituting  $\frac{b}{e}$  from (39) (with  $\xi_f = 0$ ) in (56), we find the following inequality:

$$\begin{aligned} & \frac{2(\frac{b}{e})^2 e^{-w_f^2(\frac{\pi}{2})}}{w_f^3(\frac{\pi}{2}) + 3w_f(\frac{\pi}{2})} \int_0^{w_f(\frac{\pi}{2})} e^{-w^2} dw = \frac{2[w_f^2(\frac{\pi}{2}) + 2]^2 e^{w_f^2(\frac{\pi}{2})}}{w_f^3(\frac{\pi}{2}) + 3w_f(\frac{\pi}{2})} \int_0^{w_f(\frac{\pi}{2})} e^{-w^2} dw \\ & \geq \frac{2[w_f^2(\frac{\pi}{2}) + 2]^2 e^{-w_f^2(\frac{\pi}{2})}}{w_f^3(\frac{\pi}{2}) + 3w_f(\frac{\pi}{2})} \int_0^{w_f(\frac{\pi}{2})} e^{-w_f^2(\frac{\pi}{2})} dw = \frac{2[w_f^2(\frac{\pi}{2}) + 2]^2}{w_f^2(\frac{\pi}{2}) + 3} > 2 , \end{aligned} \quad (57)$$

thus showing that

$$\left. \frac{\partial^2 s}{\partial \gamma^2} \right|_{\gamma=\frac{\pi}{2}} < 0 . \quad (58)$$

It should be stressed that (58) does not depend on  $b$ . We conclude that the distance from the center presents a local *maximum* at the equator, thus showing that our naive expectations from the analysis in Section 3 were unfounded.

Let us now consider geodesics joining points symmetrically placed with respect to the equator,  $(w_0, \xi_0)$  and  $(w_0, -\xi_0)$ , and having  $\dot{\varphi} = 0$ . For symmetry and differentiability reasons, such geodesics must intersect the equatorial plane orthogonally, with respect to the metric

$$\frac{2}{m}dw^2 + \frac{1}{2m} \left(\frac{e}{b}\right) \frac{e^{w^2}}{\cos \xi} d\xi^2 . \quad (59)$$

The orthogonality condition fixes the parameter  $\beta$  in (33) and (34):

$$\beta = e^{-w_c^2} , \quad (60)$$

where  $w_c$  is the  $w$  coordinate of the intersection of the geodesic with the equatorial plane. We shall now consider the portion of the geodesic starting orthogonally to the equatorial plane from  $(w_c, 0)$  and ending in  $(w_0, \xi_0)$ , whose length will obviously be half that of the complete geodesic starting at  $(w_0, -\xi_0)$  and ending in  $(w_0, \xi_0)$ . The signs in (31) and (34) are fixed by the initial conditions, giving

$$\epsilon q = +1 . \quad (61)$$

In principle, the considered portion of geodesic in the northern hemisphere could have  $\dot{w} > 0$  or  $\dot{w} < 0$ . But the latter does not, in fact, exist, as one would have

$$\beta - e^{-w^2} < 0 , \quad (62)$$

due to the fact that  $w_0 < w_c$  for  $\dot{w} < 0$ : From (33), such a possibility is incompatible with the equation for the geodesic trajectory. We conclude that the unique geodesic joining  $(w_0, -\xi_0)$  and  $(w_0, \xi_0)$  cuts orthogonally the equatorial plane at  $(w_c, 0)$ , with  $w_c < w_0$ , and exhibits the monotonic behaviour  $\dot{w} > 0$  and  $\dot{\xi} > 0$  [from (61) and (31)] in the northern hemisphere.

Such a geodesic is the natural generalization of a straight line parallel to the rotation axis in the Newtonian case: Both can be defined as non-twisting ( $\dot{\varphi} = 0$ ) geodesics that intersect the equatorial plane orthogonally. We shall now show that the geodesic thus introduced is completely contained in the three-dimensional body bounded by the surface  $t = \text{const.}$ ,  $p = 0$ . To this end, we consider the pressure  $p$  as a function of a point in the geodesic; from (3),

$$2\frac{\kappa_0}{m}p(s) = w^2(s) + 2 - \frac{b}{e} \cos \xi(s)e^{-w^2(s)} . \quad (63)$$

By differentiating (63) with respect to the distances from the starting point  $(w_c, 0)$  along the portion of the geodesic in the northern hemisphere (we denote the derivative by a dot), we find

$$2\frac{\kappa_0}{m}\dot{p} = (2w + 2\frac{b}{e} \cos \xi w e^{-w^2})\dot{w} + \frac{b}{e} \sin \xi e^{-w^2} \dot{\xi} ; \quad (64)$$

but, due to the inequalities  $\dot{w} > 0$  and  $\dot{\xi} > 0$  for the northern portion of the geodesic, and the fact that  $2w + 2\frac{b}{e}\cos\xi we^{-w^2} > 0$  and  $\frac{b}{e}\sin\xi e^{-w^2} > 0$ , we conclude that

$$\dot{p} > 0 . \tag{65}$$

As a consequence, the pressure along the geodesic increases from  $(w_c, 0)$  to the endpoint  $(w_0, \xi_0)$ . Conversely, traversing the geodesic in the opposite sense [starting from  $(w_0, \xi_0)$  and heading towards  $(w_c, 0)$ ] corresponds to decreasing values of  $p$ . As the pressure decreases towards the interior in the solution under consideration, it is clear that a geodesic of the type just introduced which starts at a point in the surface ( $p = 0$ ) in the northern hemisphere has  $p < 0$  at all other points in the northern hemisphere. By symmetry, all other points of the geodesic in the southern hemisphere have  $p < 0$ , except for the final point, where  $p = 0$ . Thus, a geodesic of the type considered has only two points of intersection with the bounding surface, thus maintaining in the present fluid configuration the classical (Newtonian) result for the intersection of straight lines parallel to the rotation axis with the boundary  $p = 0$ .

We have found that all the criteria we have considered reproduce the convexity properties of Newtonian configurations, in spite of the peculiar behaviour of the boundary surface, as analyzed in Section 3. It is clear that the standard Euclidean relations among convex bodies and their bounding surfaces, [6], [7], [8], do not hold for a general Riemannian geometry, dynamically prescribed by Einstein's equations.

## 6 Conclusions

We have analyzed some geometric features related to the shape and convexity properties of a self-gravitating body of perfect fluid in stationary rotation, as given by the exact solution [1]. Our analysis of the boundary ( $t = \text{const.}$ ,  $p = 0$ ) shows that for some rotation rates there appear features that would be interpreted in the Euclidean case as non-Newtonian. However, by looking at the behaviour of geodesics in the three-dimensional fluid within the bounding surface, the analog of the Newtonian results under consideration is obtained. The technique to show them is a detailed analysis of the spatial geodesics within the fluid, and specifically the introduction of a family of geodesics which generalize the straight lines parallel to the axis of rotation in the Newtonian case.

## 7 Acknowledgments

We thank L. Fernández-Jambrina, L. M. González-Romero, and F. Navarro for discussions. Financial support from Dirección General de Enseñanza Superior e Investigación Científica (Project PB95-0371) is gratefully acknowledged.

## References

- [1] D. Kramer, *Class. Quantum Grav.* **1**, L3-L7 (1984)
- [2] D. Kramer, *Astron. Nach.* **307**, 309-312 (1986)
- [3] H. Lamb: *Hydrodynamics* (reprinted by Dover, New York, 1945)
- [4] L. Lichtenstein, *Sitzungsb. d. Preuß. Akad. d. Wiss.*, 1120-1135 (1918)
- [5] L. Lichtenstein: *Gleichgewichtsfiguren rotierender Flüssigkeiten* (Springer, Berlin, 1933)
- [6] J. Hadamard, *J. Math. Pures Appl.* (5)**3**, 331-387 (1897); (5)**4**, 27-73 (1898)
- [7] T. Bonnesen and W. F. Fenchel: *Theorie der konvexen Körper* (Springer, Berlin, 1934)
- [8] S. S. Chern and R. K. Lashof, *Am. J. Math.* **79**, 306-318 (1957)